The Value of Tropical Forests to Hydropower

Rafael Araujo*

October 2, 2023

Abstract

Tropical forests have a significant impact on rainfall patterns at a continental scale, thereby influencing water supply for energy generation of hydropower plants. I develop a method to value this ecosystem service using an econometric climate model that connects tropical deforestation with rainfall. As an application, I estimate the impact that Amazon deforestation has on the power generation capacity of the Teles Pires hydropower plant in Brazil, one of the ten largest plants in a country where hydropower is the main source of energy. In an ex-post analysis, I map the currently deforested regions in the Amazon with the highest restoration values for the hydroelectric. In an ex-ante analysis, I map the potential cost of deforesting Indigenous Territories. The results provide evidence of the importance of the ecosystem services of tropical forests to the energy sector.

JEL: *Q57, L94, Q23, Q25, Q54*

Keywords: *Deforestation, Amazon, Energy, Climate, Hydropower plants*

1 Introduction

Tropical forests are responsible for a significant share of the rainfall in South America, Africa, and Asia (Spracklen et al., 2012; Lawrence and Vandecar, 2015), locations with a high presence and/or a high potential for hydropower plants (HPs) (IEA, 2021; Fan et al., 2022; Anderson et al., 2018). This rainfall supply mechanism extends even to hydropower plants located hundreds or thousands of kilometers away from the forests (Spracklen et al., 2012). Deforestation, therefore, has a continental-scale impact on hydropower, which is a renewable energy source that can significantly increase energy capacity, particularly in developing countries (WWAP, 2012; Agency, 2009; IEA, 2021). Valuing ecosystem services, such as rainfall supply, composes an agenda of accounting for the natural capital in economic models and is a key step in designing environmental protection policies and nature-based solutions (Ferraro et al., 2020; Johnson et al., 2021; Dasgupta, 2021). Nonetheless, assessing the value of nature remains challenging due to the complex interactions and externality effects from climate and ecosystem models that need to be connected with models from other areas of study, such as energy generation.

In this paper, I develop a data-driven approach to estimate the value of tropical forests for energy generation of hydropower plants (HPs) through a chain of effects: deforestation affects rainfall, rainfall affects river flow, and river flow affects energy generation. The value of the forgone energy in a HP caused by a counterfactual deforestation scenario allows me to measure the value of different regions of the forest for the HP. This chain of effects starts with the crucial role that tropical forests play in continental rainfall, where the transpiration of trees contributes to increase atmospheric humidity and subsequent downwind rainfall (Wunderling et al., 2022). To model this mechanism, I develop an econometric climate model that connects a deforestation scenario with rainfall.

I build atmospheric trajectories that cover the forest using data on wind speed and direction. Along the trajectories, I quantify the extent of forest exposure encountered by each trajectory. I then estimate the effect that this measure of upwind exposure to the forest has on downwind rainfall. The estimated parameters allow me to build, for each possible scenario of deforestation, a counterfactual rainfall measure. The identification of the climate model relies on short-run variation of wind speed and direction compounded along continental trajectories of humidity transport. In the next step, I estimate the effect of rainfall on the river flow with a predictive model and compute the effect of river flow on the energy generation potential with a log-log specification based on physics (Stickler et al., 2013). The forgone energy value from reduced rainfall can be interpreted as the willingness to pay for forest conservation and/or restoration. Finally, I map the regions of the forest with

the highest values for the HP, which are the regions that are most visited by the atmospheric trajectories upwind of the HP. This methodology not only quantifies the willingness to pay for conservation and restoration but also provides targeted mapping for conservation and restoration efforts tailored to individual HPs.

In a first application, I investigate the impact that the deforestation of the Amazon Rainforest since the 1980's has on the energy generation capacity of the Teles Pires HP in Brazil. As 64% of Brazil's installed capacity comes from hydropower,[1] the country's electrical matrix is particularly susceptible to rainfall changes. Teles Pires, located in the state of Mato Grosso, stands as one of the ten largest hydropower plants in Brazil and its water supply is heavily influenced by deforestation due to its proximity to the Amazon Rainforest. It started its operation in 2015 and in 2021 entered a special stand still program with the National Development Bank (BNDES) to temporarily suspend the payment of financing agreements due to a water crisis.

I find that the Amazon deforestation generates an average decrease of rainfall of 13% and 8% of the historical average in the state of Mato Grosso in the dry and wet seasons, respectively. For the specific location of the Teles Pires plant, this decrease ranges between 6% and 10%. The impact of this decrease in rainfall amounts to an average decrease in potential energy generation between 2.5% and 10%, with extreme scenarios exceeding 17%. For the hydropower plant, this decline in energy generation translates to an average annual loss of approximately USD 21 million per year, representing around 10% of the HP's annual revenue. This application shows how the model can be used to compute ex-post effects of deforestation.

In a second application, I compute an ex-ante effect of deforestation. The Indigenous Territory of Mundurucu is located both *downstream* and *upwind* of Teles Pires, thus the territory provides water to the HP via atmospheric circulation and is affected by river flow changes caused by the plant. In this second counterfactual exercise, I estimate the value of the forest in the Mundurucu territory for Teles Pires. In this counterfactual scenario, I completely deforest the Indigenous Territory and find that the Mundurucu territory provides to Teles Pires an average positive externality via rainfall of USD 2.3 million per year, representing approximately 1% of the hydropower plant's annual revenue.

This paper adds to an agenda of valuing ecosystem services (Ferraro et al., 2020; Johnson et al., 2021; Dasgupta, 2021), that for tropical forests are often constrained to valuing the forests as a carbon sink (Franklin Jr and Pindyck, 2018; Araujo et al., 2020). By incorporating the externality effect of forests on rainfall, this research expands the understanding

---

[1]Brazilian Energy Balance 2020, available at `epe.gov.br/pt/publicacoes-dados-abertos/publicacoes/balanco-energetico-nacional-2020`, page 20, accessed 01/20/2023.

of the cost-benefit analysis of deforestation policies studied so far (Souza-Rodrigues, 2019; Jung et al., 2022; Simonet et al., 2019; Assunção et al., 2022, 2019, 2020; Araujo et al., 2023). This paper also relates with studies that connect the mechanism of forest and rainfall with agriculture (Leite-Filho et al., 2021; Araujo, 2023; Grosset et al., 2023) and human consumption (Núñez et al., 2006).

The methodology can be applied in different regions with the presence of tropical forests, such as South America, Indonesia, and Africa. Since the effect of deforestation on precipitation goes beyond borders, this model can be used to measure externalities among countries, much in the same way that transboundary water treaties and agreements address the use of rivers (Sigman, 2002; Ambec et al., 2013; Olmstead and Sigman, 2015). The climate model can also be applied in a range of different sectors, such as, agriculture and water supply for human consumption, and therefore be used to study allocation of scarce water resources across competing sectors (Olmstead, 2020). Tropical forests are instruments to counteract rainfall changes caused by global warming (Seneviratne et al., 2012). Measuring the importance of the forest is useful to plan conservation/restoration policies to lessen the impacts of changes in rainfall studied in the literature of adaptation to climate change in the agricultural sector (Skidmore, 2022) and economic growth (Damania et al., 2020; Barrios et al., 2010).

Methodologically, the climate model relates to a long standing literature connecting tropical forest and climate. The transpiration and water recycling mechanism was first explored by Salati et al. (1979). Pioneering studies connecting atmospheric circulation and the water cycle showed how the long-range atmospheric transport of water affects continental rainfall using global climate models (Shukla et al., 1990; Nobre et al., 1991), followed by regional calibrated models (Zemp et al., 2017; Wunderling et al., 2022; Staal et al., 2023, 2018). Spracklen et al. (2012) introduced a single estimation equation connecting the forest, atmospheric trajectories, and rainfall, which is most closely related to my method. Recent estimated models includes Smith et al. (2023) and Cui et al. (2022).

This paper also contributes to the existing literature on hydropower, which has primarily focused on shifts of energy sources (Crampes and Moreaux, 2001; Genc and Thille, 2011; Eyer and Wichman, 2018; Qiu et al., 2023) and entry of multiple HPs in the same basin (Moita, 2008). On the intersection of deforestation and hydropower, Stickler et al. (2013) studies effects of deforestation on the flow of a basin and its effect on energy generation using general computable models and Guo et al. (2007) studies local interactions of forest conservation and hydroelectricity. This paper departs from this literature by uncovering another layer of externalities when studying HPs in regions affected by tropical forests, explicitly isolating the variation that identifies the effect of deforestation on energy generation. On the effects of

changes in climate in energy supply, the literature has focused on rising temperatures from climate change and their consequences (Bogmans et al., 2017; Rosende et al., 2019; Ciscar and Dowling, 2014). This paper depart from this literature by exploring a mechanism that has continental/local impacts on rainfall.

Additionally, this study contributes to the literature of environmental injustice (Mohai et al., 2009; Hernandez-Cortes and Meng, 2023). Communities downstream of hydropower plants may experience adverse effects due to changes in river flow [2] and surrounding communities may not benefit in the long-run (De Faria et al., 2017). Concomitantly, depending on the patterns of atmospheric circulation, the same affected communities may also contribute to the HPs' energy generation by preserving the native vegetation of their territory and supplying water through atmospheric circulation. This scenario creates a double environmental injustice where people may not be compensated for the positive externality they generate via one ecosystem service - providing rainfall - while bearing the burden of a negative externality via another ecosystem service - changes in river flow.
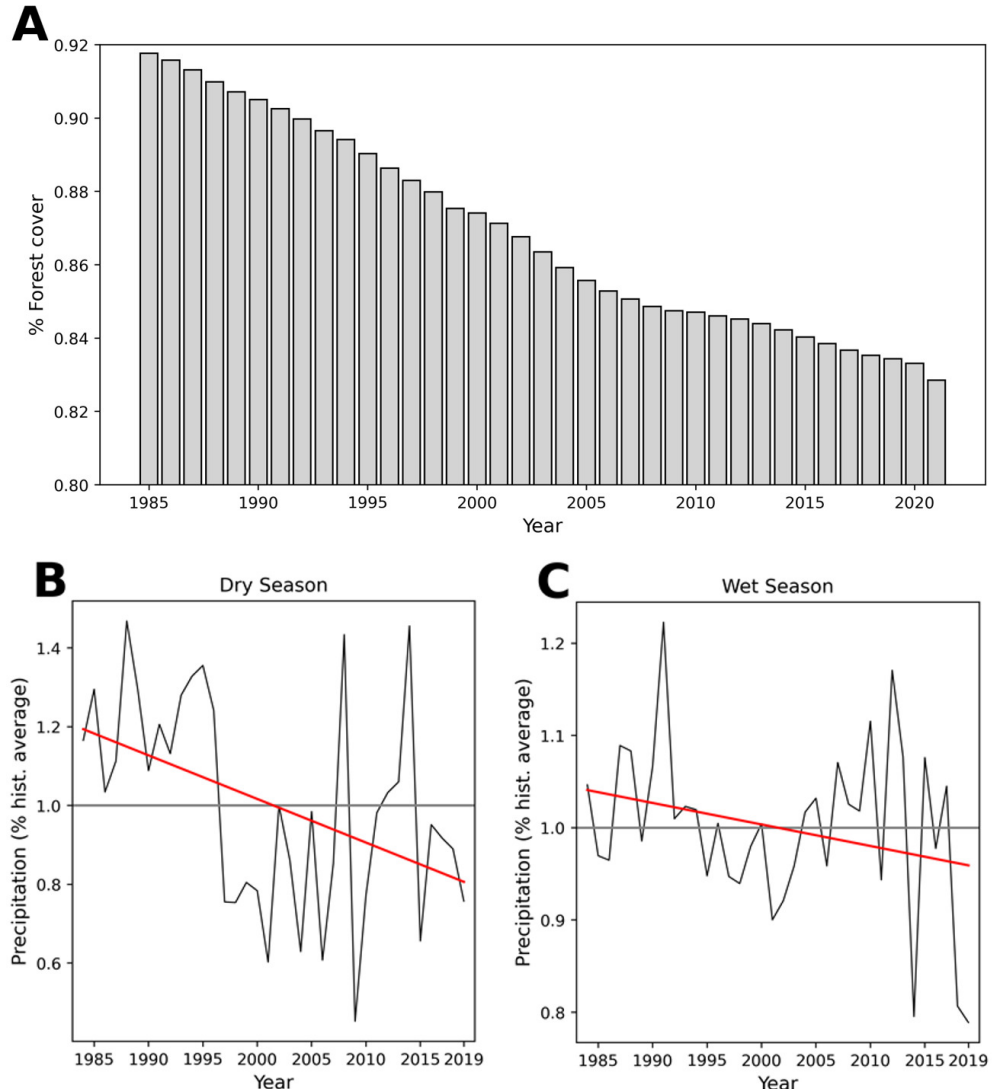
The remainder of this article is organized as follows: Section 2 describes the climate model; Section 3 describes the connection between rainfall and energy; Section 4 estimates the impact of deforestation on energy generation; Section 5 estimates the value of the ecosystem service of the Amazon forest; Section 6 estimates the value of the Indigenous Territory of Mundurucu to the HP; Section 7 concludes.

2   Climate Model: Deforestation and Rainfall

Tropical forests are an important part of the water cycle. The evaporation of the water in the oceans creates humid air parcels that are transported to continental lands. Along its trajectory, the air loses humidity via precipitation. But, on the ground, trees' transpiration recharges the air's humidity contributing to rainfall downwind. Thus, trees affect rainfall (Salati et al., 1979; Wunderling et al., 2022). The presence of tropical forest can affect rainfall in locations that are hundreds and even thousands of kilometers away from the forest, a phenomenon known in the literature as flying rivers (Marengo et al., 2018). An implication of this mechanism is that deforestation decreases rainfall. The Amazon rainforest has seen a steady decline in its forest cover in the last 4 decades (Figure 1 A), and as a consequence, there is also a steady decline in precipitation both in the dry season (Figure 1 B) and wet season (Figure 1 C) in the state of Mato Grosso, which will be the location of the application developed in this paper.

---

[2]As of 2023, most of the processes in the court system against Teles Pires HP related with downstream

Figure 1: Upwind Exposure to the Forest

This figure illustrates (A) the decline in forest cover in the Amazon region in the last 4 decades (Mapbiomas, 2022). (B) and (C) show the average precipitation in the state of Mato Grosso for the wet and dry seasons, measured as a proportion of the historical average. Notice the declining trend, which is more pronounced in the dry season (Copernicus, 2017).

To model this effect, I follow Spracklen et al. (2012) in creating a data set that connects upwind exposure to trees to downwind rainfall. The first step is to build trajectories through which these air parcels travel, a model of atmospheric transportation. The trajectories are built with data on wind speed and direction. Suppose I have an air parcel over a location ℓ (latitude and longitude) for which I am interested in modelling rainfall, then I can use the data on wind speed and direction to move one step back, that is to find where this air parcel was one hour ago. If I keep doing this, eventually I will have traced the air parcel back to the ocean.[3] Figure 2a shows an example of a back trajectory.

The second step is to create a measure of exposure of that back trajectory to the forest. This step requires forest data for all the area covered by the back trajectory, such as a binary data indicating whether a location is forested or deforested. I then count the number of forest pixels crossed by a back trajectory. For example, the back trajectory in Figure 2A will have a measure of 12 pixels of forest. I can then repeat steps one and two for different periods for all locations of interest. For example, in a different year, I could have the second trajectory depicted in Figure 2B, with a measure of 11 pixels of forest. From Figure 2, it is likely that the back trajectory in scenario A will deliver more rainfall than the back trajectory in scenario B, since the exposure to forested pixels is higher in scenario A.

As an application, in this paper I model the effect of Amazon deforestation on the rainfall of the Brazilian state of Mato Grosso, shown in Figure 4A. I collect three-dimensional data on monthly wind speed and direction from 1985 to 2020 for the entirety of South America at the resolution of 0.25° Copernicus (2017). For each month I have a three-dimensional matrix with information on wind speed and direction for each point on South America (latitude and longitude) and pressure levels varying from altitudes close to the forest canopy up to around 8000 meters. I also collect yearly data on land use for the entire Amazon from 1985 to 2020 from Mapbiomas (2022), at a resolution of 30 meters. I then upscale Mapbiomas' data to match the resolution of ERA5's data with an average filter. Figure 3A shows a sample of back trajectories for the state of Mato Grosso. See in the Appendix Table 4 for descriptive statistics and Table 3 for additional information on the data source.

To estimate the relation between forest and rainfall, denote by $r_{\ell,m,y}$ the rainfall in location ℓ, month m, and year y; $f_{\ell,m,y}$ the exposure to forested pixels along the back trajectory

---

communities are about fish deaths and lack of potable water.

[3]I compute the back trajectories up to 5 days and set pressure level to 800 hPa following Spracklen et al. (2012). Each step and output has length of 1 hour. Spracklen et al. (2012) uses a smaller panel data (2001-2007) with a lower spatial resolution (100°) but with a higher temporal resolution (hourly). As I employ a fixed-effect estimator, I need a long panel to generate enough variation of deviations along long-term transportation patterns. Also, as I want to study the effect of deforestation on Teles Pires, I opted for a higher spatial resolution.

started in ℓ, or the upwind exposure to the forest; $x_{\ell,m,y}$ the length of the back trajectory on land, to control for the fact that longer trajectories mechanically present a higher count of upwind exposure to the forest. The effect of deforestation on rainfall is given in Expression 1

$$r_{\ell,m,y} = \alpha + \beta_m f_{\ell,m,y} + \gamma x_{\ell,m,y} + \epsilon_{\ell,m,y} \tag{1}$$

As the back trajectories are long, the $f_{\ell,m,y}$ measure is dominated by forest pixels that are far away from location ℓ. Therefore, it is unlikely that local shocks to ℓ can affect the count $f_{\ell,m,y}$. For example, the construction of a road in location ℓ could concomitantly affect local deforestation and rainfall (perhaps through changes in local temperature). In this case there could be variables in the error term of Expression 1 that correlates with the exposure to the forest variable ($f_{\ell,m,y}$). Nonetheless, the atmospheric trajectories that are relevant for the mechanism are hundreds or even thousands of kilometers long, in a way that local changes in deforestation – for example, in a 25 kilometers range – will have a small numerical impact in the total exposure to the forest.

It is important not to include mediators or bad controls (Wooldridge, 2005), such as temperature, since the upwind exposure to the forest can affect temperature at ℓ. The identification of the model relies on the variation of the back trajectories and therefore on the variation of the wind data. Furthermore, the mechanisms behind the link between transpiration and humidity transport (Salati et al., 1979; Spracklen et al., 2012) provide further evidence of the causal interpretation of Expression 1. Notice that for each location-month I build one back trajectory generated by the prevailing winds of that month. To build the exposure to forest pixels for each location-month I overlap the coordinates of the back trajectory with the land use data (see Figure 2).

There are many options of atmospheric transport models relying on data of wind speed and direction that are then integrated to build atmospheric trajectories. The differences among the models are the spatial resolution, the temporal resolution and the integration method. Alternative models from the economics literature on pollution make use of atmospheric models with greater temporal resolution (Hernandez-Cortes and Meng, 2023; Miller et al., 2017). This is necessary since a pollution source, such as fires, is usually short-lived. But the transportation of humidity from the ocean is a continuous process, which allows me to leverage monthly trajectories patterns and thus explore longer panels.

Figure 3B shows the results of this estimation for different sets of fixed effects with stable results across specifications (Table 1). As expected, the estimated β_m coefficients are all positive, meaning that upwind exposure to the forest increases downwind rainfall. As Figure

7
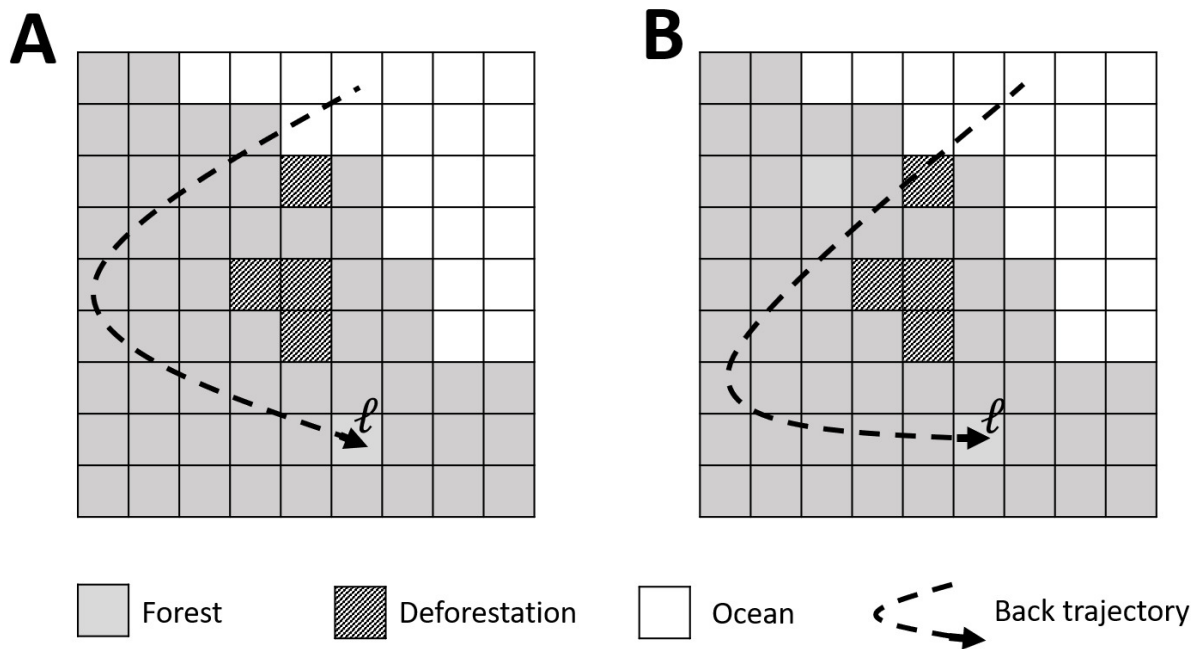
3B shows, the effect of forest exposure on rainfall is lower in the dry season. Notice that Expression 1 is an equation in levels, connecting rainfall levels to the exposure to the forest variable. Statistically, as rainfall is higher in the wet season (see Table 4 in the Appendix) , it is expected that the overall effect of vegetation on rainfall would be higher in the wet season. From a mechanism perspective, the transpiration of trees varies along the year, being higher in levels in the wet-season, even though the ratio of precipitation of transpiration origin divided by the total precipitation is lower (Costa et al., 2012).

To understand the magnitude of the estimated effects, I explore a counterfactual where there would not have been deforestation in the Amazon since 1985, the first year I have data on land use. As atmospheric trajectories vary year to year, to generate a counterfactual change in rainfall I compute counterfactual changes for all years in the data. For visualization purposes I also compute the average across years. I assume that all the atmospheric trajectories of the last decades offer a good approximation of the distribution of possible atmospheric trajectories and that an average of these trajectories is the best predictor of future behavior. In Section 4, I discuss how year-to-year variation in atmospheric trajectories affect the counterfactual exercises of potential energy generation.

Figures 3C and 3D show the impact that the accumulated deforestation of the Amazon since 1985 has on the total rainfall of the dry season - April to August - and the wet season - September to March - measured as a proportion of the historical average. The accumulated Amazon deforestation generates a decrease of rainfall of 13% and 8% of the historical average in the state of Mato Grosso in the dry and wet seasons, respectively. Some regions face an effect of more than 25% in the dry season and other regions face an effect of more than 14% in the wet season.

There are other potential mechanisms connecting deforestation and rainfall. In this paper, I focus only on one mechanism, of deforestation affecting rainfall via changes in transpiration and its transport via atmospheric circulation. In the model, I only capture effects that can be explained by the combined variation of wind changes and deforestation. Given the length and direction of back trajectories shown in Figure 3A, most of the variation of the upwind exposure to the forest comes from deforestation outside of the Teles Pires river basin and downriver from the plant, therefore it does not account for other mechanisms that may result in decrease of river flow in the basin, such as potential large upriver irrigation projects. Additionally, as noted in Leite-Filho et al. (2021) and Smith et al. (2023), even at a local level deforestation has additional negative impacts on rainfall. Thus my results should be interpreted as a lower bound on the effects of deforestation on rainfall, river flow, and energy generation.

Figure 2: Upwind Exposure to the Forest

This figure illustrates the construction of the upwind exposure to forested pixels. Consider a location ℓ, in which we are interested in modelling the rainfall. In A and B, the dashed black line represents a back trajectory of atmospheric transport from ℓ to the Ocean. Each trajectory visited different pixels along the way. Specifically, in A the back trajectory visited 12 pixels of forest and in B the back trajectory visited 11 pixels of forest. These numbers are what I denoted by $f_{\ell,m,y}$ in Expression 1

3   Teles Pires: Rainfall and Energy Capacity

The Teles Pires HP started operating in 2015. As a run-of-river plant, it is characterized by a limited capacity of water storage that thus relies heavily on the river flow. This type of HP can change environmental costs associated with HPs (Assunção et al., 2017; Bertas-soli Jr et al., 2021), since its does not require the flooding of large portions of land for the construction of a reservoir. Teles Pires has an installed capacity of 1,820 MW, sufficient to supply a population of 5 million people. Figure 4A shows the location of the HP and of the Teles Pires' basin. I use panel data to estimate the climate model (Expression 1), leveraging spatial and temporal variation in the data. But to study counterfactuals in Teles Pires, once I have estimated the parameters, I apply them to the data at the location of the Teles Pires HP, which given the resolution of my data, is a time series. The effect of deforestation on rainfall calculated in Section 2 for the location of Teles Pires generates an average decrease of rainfall of 6% and 10% of the historical average in the dry and wet seasons, respectively.

There are two steps to measure the impact that changes in rainfall have on energy generation: first, map how rainfall affects the river flow; second, map how the river flow affects potential energy generation.

I use river flow data from the National System Operator (ONS, 2022) from 2015 to 2020 and the same monthly data on rainfall that was used for the climate model, but selecting data only at the location of the plant. The model is a linear regression of the log of river flow on a month (d_m) on the accumulated 4 months rainfall (r_m), as described in Expression 2. Figure 4B shows that both variables are strongly correlated and Table 2 in the Appendix shows a R^2 of 94% for the linear regression model. In a cross-validation exercise with a year-by-year rolling window the average R^2 is of 93%. Different from the causal climate model, Expression 2 is a predictive model where I am not interested in identifying causal mechanisms of how rainfall affects river flow, but rather to build a forecast of how changes in rainfall explain changes in river flow. A predictive model has the advantage of requiring less domain knowledge for its implementation and it is easier to validate given the goal of minimizing prediction errors using cross-validation (e.g., Athey (2017)). It is important to acknowledge the limitations of this approach, in particular if changes in rainfall were enough to change the joint distribution of rainfall and river flow the predictive performance could drop in counterfactual scenarios. However, I believe the predictive model is the most suitable in this case given that my counterfactual rainfall decrease in Teles Pires is around 10%.

$$\log d_m = \alpha + \beta \left(\sum_{t=m-3}^{m} r_t \right) + \epsilon_m \tag{2}$$

To map how river flow (d_m) affects monthly potential energy generation (p_m), I follow a formula based on physics given in Expression 3 (Stickler et al., 2013). This expression is not estimated since the elasticity of river flow on potential energy generation is known to be one.

$$\log p_m = \log d_m + \psi_m \tag{3}$$

Expression 3 is a specification from physics. The Gravitational Potential Energy (GPE) is given by $GPE = mgh$, where m denotes mass, g the acceleration of gravity, and h is the height (see e.g., Halliday et al. (2013)). In the hydropower case, water (mass m) is stored at a higher elevation than the turbines (the h variable). Additional heterogeneity, such as waste from different turbines, are captured by additional (empirical) constraint parameters, say k, extending the equation to $GPE = kmgh$. Nonetheless, taking logs we have $\log GPE = \psi + \log m$, where ψ is a combination of characteristics constant for a HP (g, k, h).

While I am modeling changes in potential energy generation, as Teles Pires is a run-of-river plant, the connection between potential and actual energy generation is very close. A regression of the log of energy generation on a constant and the log of river flow yields a elasticity of 0.91 (standard deviation of 0.05). The estimated elasticity is close to one and statistically we cannot reject the hypothesis that it is one, as expected by the elasticity imposed in Expression 3 that connects river flow with potential energy generation.
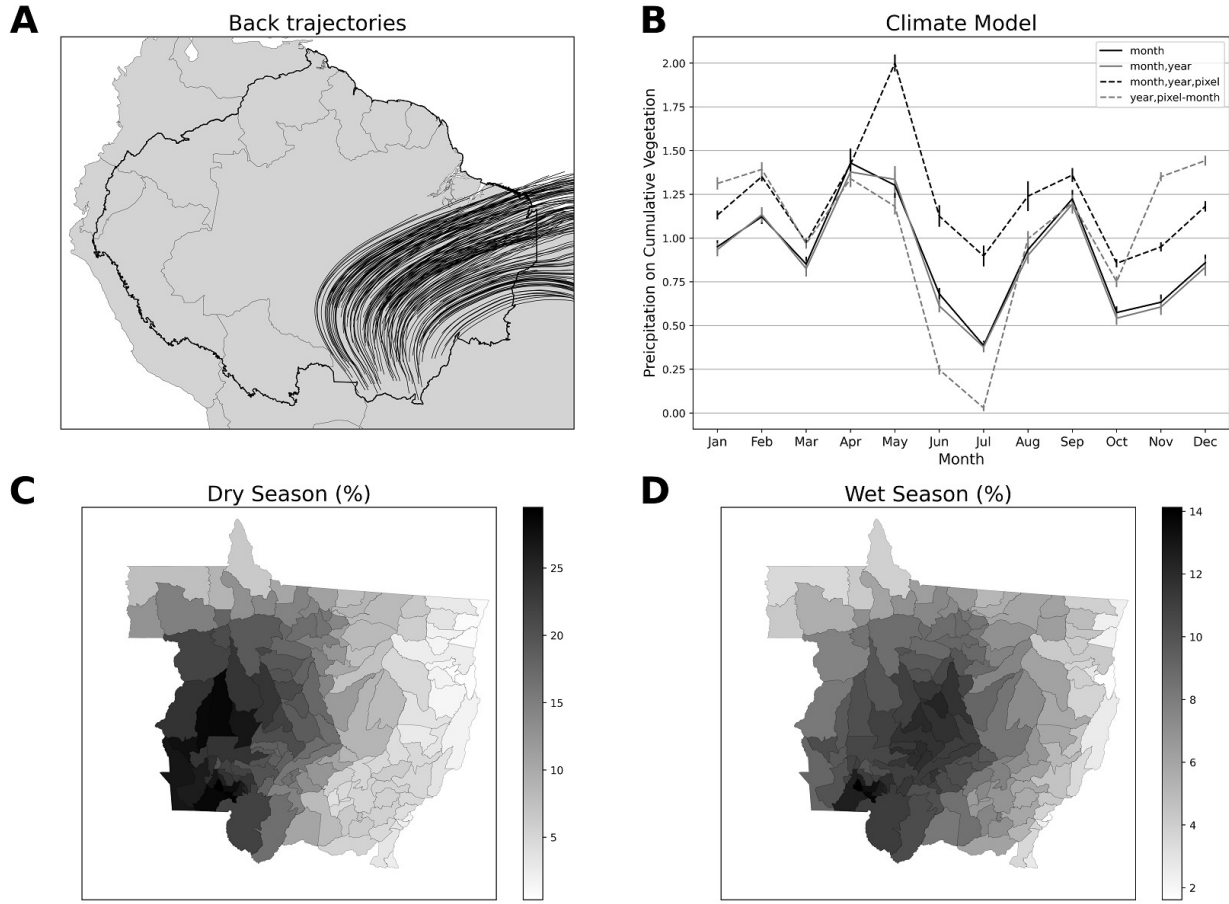
Once the β parameter is recovered from Expression 2, I can compute the effect of rainfall changes on potential energy generation in a closed form Expression 4

$$\frac{\Delta p_m}{p_m} \approx \beta \Delta \left(\sum_{t=m-3}^{m} r_t \right) \tag{4}$$

4 Teles Pires: Deforestation and Energy Capacity

To compute the impact that the Amazon deforestation has on the energy capacity of the HP, I combine: Expression 4; the difference between observed and counterfactual rainfall computed in Section 2; and the estimated parameter β of Table 2. I generate a difference between observed and counterfactual rainfall using the atmospheric trajectory data for each month of year since 1985 up to 2020. The idea is that all the atmospheric trajectories of the last four decades offer a good approximation of the distribution of possible atmospheric trajectories. Then, for each pair of month and year atmospheric data I compute $\frac{\Delta p_m}{p_m}$, the

Figure 3: Deforestation and Rainfall

(A) the black lines show a sample of the atmospheric back trajectories for February 2015. (B) shows the result of estimating Expression 1 for different sets of fixed effects. This regression captures the effect that upwind exposure to the forest has on downwind rainfall. The values of this graph are shown in Table 1 in the Appendix. the vertical bars shows the 95% confidence interval with standard errors clustered at the pixel level. (C) and (D) show the decrease in rainfall as the result of Amazon deforestation for the dry season and wet season, respectively, measured as a proportion of the historical average.

percentage change in energy capacity, as described by Expression 4.

Figure 4C shows the result of this exercise. As in Section 2 and Figures 3 C and D, the counterfactual I am considering is one where there would be no deforestation. The gray lines show the loss in potential capacity for each year of atmospheric trajectory data and the black line shows the average across the years. The average effect across years indicates a loss of capacity between 10% and 2.5% due to the cumulative Amazon deforestation. The average effect, nonetheless, is far from the extreme scenarios in which the effect can be as large as 17.5%. These large effects would occur in the years that atmospheric trajectories are such that they are highly exposed to deforested regions.

5 The Value of the Forest for Teles Pires

To compute the value of the forest for Teles Pires, I use a partial equilibrium analysis. I multiply the average loss of energy capacity by a monthly average of the price of energy from 2015 to 2020 (CCEE, 2022)[4]. To compute the average loss of energy capacity I multiply the estimated effects of Figure 4C (the gray lines) by the monthly potential energy generation and take the average.[5] The result indicates an expected loss of USD 21 million per year, which can be interpreted as the HP's willingness to pay for conservation/restoration policies. This calculated loss, which is essentially price times quantity, is suitable for my application because the marginal cost of the HP operation is negligible (Edenhofer et al., 2011) and Teles Pires is a price taker, since it accounts for a little more than 1% of the installed capacity in Brazil. Nonetheless, a counterfactual scenario without deforestation could impact other HPs and other sectors, changing the overall demand and supply of energy in Brazil. That would require a general equilibrium model which is not the goal of this paper (see e.g., (Jahns et al., 2020; Ferreira et al., 2015)).

If thermal power from coal or natural gas were used to compensate for the average annual loss, it could result in an emission of 347,000 tCO_2 per year (IEMA, 2022). This represents a conservative estimation of indirect emissions, as negative rainfall shocks are likely to affect multiple hydropower plants simultaneously. Considering a social cost of carbon at USD

---

[4]For this exercise I use the Price for Settlement of Differences (PLD). Possible alternatives are: Marginal Cost of Expansion computed by the Energy Research Office (EPE), for which the average deviates from the average PLD by less than 1%; Marginal Cost of Operation computed by the ONS which averages 20% higher than the PLD.

[5]When the flow of the river is already at the plant's full capacity, the benefit of more rainfall is zero. For Teles Pires, I take full capacity to be achieved with a river flow of 4,778 m^3/s, the maximum monthly average river flow. I then cap the value of rainfall to the maximum that Expression 2 predicts a flow of 4,778. The monthly potential generation is computed as the maximum energy capacity times the proportion of average monthly river flow to maximum capacity.

50 per tCO_2 (EPA, 2016), the reduced rainfall and the consequent shift from hydroelectric power would lead to an annual indirect cost of USD 17.35 million. This value is almost as large as the direct impact of reduced rainfall on Teles Pires' revenue of USD 21 million. This aligns with the results of Qiu et al. (2023), that found that in the western region of the United States the costs associated with emissions resulting from drought-induced shifts from hydro to fossil fuel generation can increase costs up to 2.5 times. Additionally, greenhouse gas emissions from hydropower plants are primarily caused by the decomposition of vegetation in reservoirs (Fearnside, 2005; Demarty and Bastien, 2011). Consequently, a decrease in energy capacity for a given HP can also elevate the ratio of potential greenhouse gas emissions per unit of energy.

Given an expected loss of USD 21 million per year and a total accumulated deforestation of 690,000 km^2 between 1985 and 2020, one could compute that the present value of the forest for Teles Pires would be of USD 612 per km^2.[6] However, this computation does not consider that only some areas of the forest affect Teles Pires via the atmospheric transport mechanism.

To distribute the willingness to pay for conservation only among those pixels that affect Teles Pires, I map which pixels in the Amazon has been visited (or flown over) by a trajectory arriving at Teles Pires. These are the painted pixels in Figure 4D. The Amazon area that influences rainfall in Teles Pires has 177,500 km^2 of deforestation and thus the present value of restoration of these areas for Teles Pires would be of USD 2,382 per km^2.
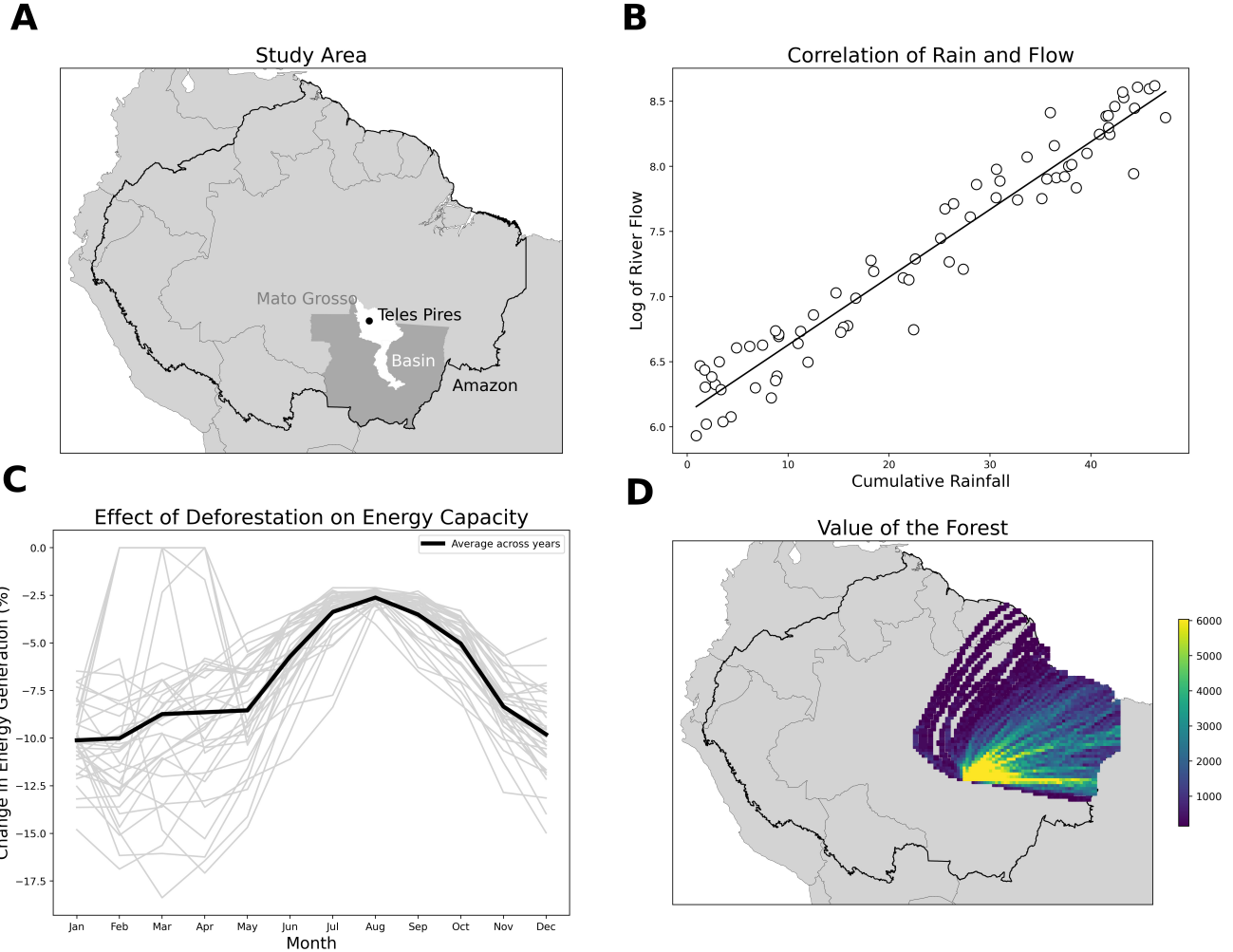
To further refine this distribution, first, I map how many times each pixels has been visited, which measures how much exposure Teles Pires has to each upwind pixel; second, I divide the willingness to pay in proportion to how many times each deforested pixel is visited. The result is shown in Figure 4D. In this last step, the mean forest value is of USD 2,037 per km^2. With 10% of them getting more than USD 4,100 and 5% of them more than USD 6,000. The average land price in the Northeast of the Brazilian Amazon is USD 100,500 per km^2 (Markit, 2021). Assuming that the land price represents all future stream of net benefits from the land, the externality cost of only one HP could buy off 2% of the private net benefits of deforestation.

6 Downstream but Upwind: Indigenous Territories

The approach described so far also allows for an ex-ante assessment of the cost of deforesting areas in the Amazon. As an application, I build a counterfactual where I deforest the entire

---

[6]Using a discount rate of 0.05: (USD 21,147 million/ km^2 690,621)/0.05
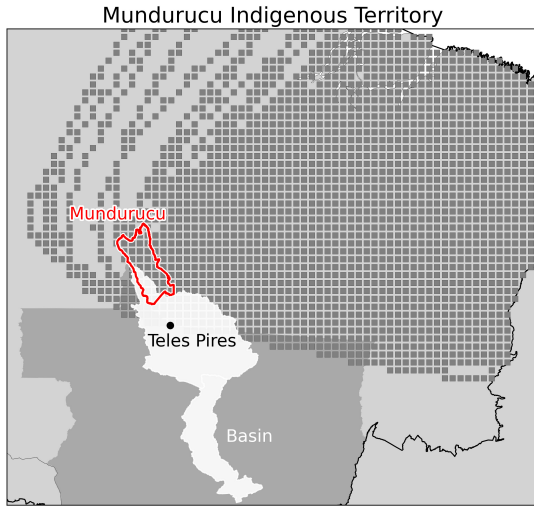
Figure 4: Deforestation and Energy Generation

A

Study Area

B

Correlation of Rain and Flow

C

Effect of Deforestation on Energy Capacity

D

Value of the Forest
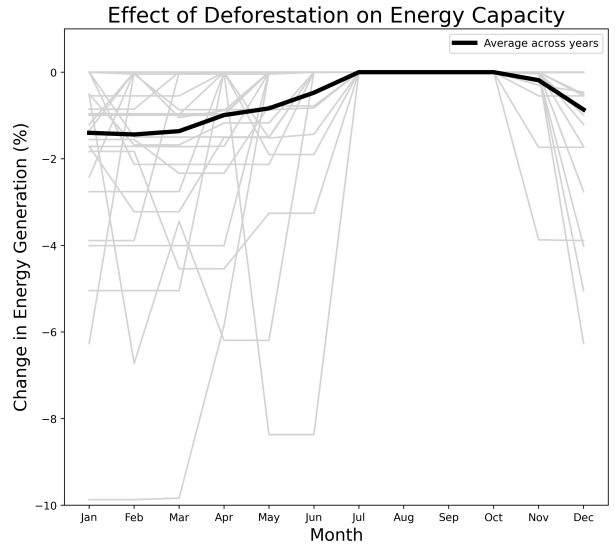
(A) shows the location of the Mato Grosso state, the Teles Pires hydropower plant, the Teles Pires river basin, and the Amazon Rainforest. (B) shows the correlation between the four months cumulative rainfall and the log of the river flow. (C) shows the effect of Amazon deforestation on the energy capacity of Teles Pires. Each gray line corresponds to the counterfactual energy capacity using atmospheric trajectories of a different year from 1985 to 2020. The black line shows the average effect of the gray lines. A zero effect occurs when the observed river flow already gives the plant full operational capacity. (D) shows the value of the forest as described in Section 5, measured in USD as the present value of 1 km^2 of forest. The values were capped at the 95% percentile for better visualization.

15

Figure 5: Deforestation in Mundurucu and Energy Generation

A

Mundurucu Indigenous Territory

B

Effect of Deforestation on Energy Capacity

(A) shows the location of the Mundurucu Indigenous territory overlapped with Figure 4 (A) and (D). (B) shows the effect of Mundurucu deforestation on the energy capacity of Teles Pires. Each gray line corresponds to the counterfactual energy capacity using atmospheric trajectories data of a different year from 1985 to 2020. The black line shows the average effect of the gray lines. A zero effect occurs when the observed river flow already gives the plant full operational capacity.

Indigenous Territory of Mundurucu (Figure 5A). This territory of 24,000 km^2 is predominantly covered in native vegetation. It is located both downstream and on the surrounding areas of Teles Pires. Thus, it can be affected by necessary relocation and changes in the downstream river flow. Concomitantly, given the patterns of atmospheric circulation in the region, the Mundurucu territory provides rainfall to the downwind Teles Pires HP, a positive externality of the forest cover.

To quantify the magnitude of this positive externality from the Mundurucu territory I run a counterfactual exercise where the entire terrritory is deforested. I then go through all the steps of the previous counterfactual, mapping the deforestation effect on rainfall, how it changes river flow and energy generation, and finally valuing this change in energy generation.

Figure 5B shows the loss of energy generation, in a similar way as in Figure 4C . As in this exercise the area considered is smaller than the previous one, the effects across months are also smaller, with the loss on the wet season being mostly around 0%-2%. The average annual loss amounts to USD 2.4 million, which can be seen as the willingness to pay of the HP to preserve the forest cover of the Indigenous Territory.

16

This type of setting shows a case where multiple ecosystem services can compose. Downstream peoples being affected by changes in an ecosystem service - river flow - while affecting other ecosystem service - rainfall supply.

7   Conclusion

I develop a data-driven approach to estimate the value of the ecosystem service provided by tropical forests in maintaining rainfall regimes for hydropower plants. I present an econometric climate model that connects a deforestation scenario with changes in rainfall. I then connect this climate model with a predictive model of how rainfall affects river flow and a model from physics of how river flow affects potential energy generation. These three steps generate the estimated lost potential energy generation due to deforestation for a HP. Finally, I show how it is possible to use the climate model to determine which specific locations in the forest the HP is most exposed to and therefore which locations have a higher value for the HP for conservation and/or restoration.

The contribution share of the Amazon rainforest for its own rainfall varies between 10% and 45% depending on the region, with an average share of 35%. Outside the Amazon basin, the contribution of the Amazon rainforest to some regions of South America can also be high, particularly on the River Plate basin it averages 17% (Zemp et al., 2017; Costa et al., 2012). Together, both basins account for 70% of the installed hydropower capacity in Brazil.

As an application, I study the effect of the Amazon deforestation on the energy capacity of Teles Pires. I first show that, in the state of Mato Grosso, where Teles Pires is located, Amazon deforestation has had an average effect of decreasing rainfall by 13% in the dry season and 8% in the wet season. This effect amounts to an average decrease in potential energy generation of 10% in some months with extreme scenarios reaching as much as 17%. The average year loss amounts to USD 21 million per year, which can be seen as a willingness to pay for conservation/restoration policies. Distributing this value proportionally among the locations in the Amazon that Teles Pires is most exposed to results in an average present value for the forest of USD 2,037 per km^2, enough to buy off 2% of the private benefits of the deforested land.

It is also possible to build an ex-ante assessment of the impact of deforestation on energy generation. I explore the counterfactual where I completely deforest the Indigenous Territory of Mundurucu, a territory located both downstream and upwind of Teles Pires. The deforestation of Mundurucu alone would cost USD 2.4 million per year for Teles Pires.

References

Agency, I. E. (2009). *World energy outlook*. OECD/IEA Paris.

Ambec, S., Dinar, A., and McKinney, D. (2013). Water sharing agreements sustainable to reduced flows. *Journal of Environmental Economics and Management*, 66(3):639–655.

Anderson, E. P., Jenkins, C. N., Heilpern, S., Maldonado-Ocampo, J. A., Carvajal-Vallejos, F. M., Encalada, A. C., Rivadeneira, J. F., Hidalgo, M., Cañas, C. M., Ortega, H., et al. (2018). Fragmentation of andes-to-amazon connectivity by hydropower dams. *Science advances*, 4(1):eaao1642.

Araujo, R. (2023). When clouds go dry: an integrated model of deforestation, rainfall, and agriculture. *Working paper*.

Araujo, R., Assunção, J., and Bragança, A. A. (2023). The effects of transportation infrastructure on deforestation in the amazon: A general equilibrium approach. *Working paper*, (10415).

Araujo, R., Costa, F., and Sant'Anna, M. (2020). Efficient forestation in the brazilian amazon: Evidence from a dynamic model.

Assunção, J., Costa, F., and Szerman, D. (2017). Power plants and deforestation: recent evidence from the amazon.

Assunção, J., Gandour, C., and Rocha, R. (2022). Deterring deforestation in the amazon: environmental monitoring and law enforcement. *American Economic Journal: Applied Economics - forthcoming*.

Assunção, J., Gandour, C., Rocha, R., and Rocha, R. (2020). The effect of rural credit on deforestation: evidence from the brazilian amazon. *The Economic Journal*, 130(626):290–330.

Assunção, J., McMillan, R., Murphy, J., and Souza-Rodrigues, E. (2019). Optimal environmental targeting in the amazon rainforest. Technical report, National Bureau of Economic Research.

Athey, S. (2017). Beyond prediction: Using big data for policy problems. *Science*, 355(6324):483–485.

Barrios, S., Bertinelli, L., and Strobl, E. (2010). Trends in rainfall and economic growth in africa: A neglected cause of the african growth tragedy. *The Review of Economics and Statistics*, 92(2):350–366.

Bertassoli Jr, D. J., Sawakuchi, H. O., de Araújo, K. R., de Camargo, M. G., Alem, V. A., Pereira, T. S., Krusche, A. V., Bastviken, D., Richey, J. E., and Sawakuchi, A. O. (2021). How green can amazon hydropower be? net carbon emission from the largest hydropower plant in amazonia. *Science Advances*, 7(26):eabe1470.

Bogmans, C. W., Dijkema, G. P., and van Vliet, M. T. (2017). Adaptation of thermal power plants: The (ir) relevance of climate (change) information. *Energy Economics*, 62:1–18.

CCEE (2022). Câmara de comercialização de energia elétrica. *www.ccee.org.br*, page acessed in 06/11/2022.

Ciscar, J.-C. and Dowling, P. (2014). Integrated assessment of climate impacts and adaptation in the energy sector. *Energy Economics*, 46:531–538.

Copernicus, C. C. S. (2017). Era5: Fifth generation of ecmwf atmospheric reanalyses of the global climate.

Costa, M. H., Borma, L., Brando, P. M., Marengo, J. A., Saleska, S. R., and V., G. L. (2012). Biogeophysical cycles: Water recycling, climate regulation. *Science Panel for the Amazon.*, Chapter 7.

Crampes, C. and Moreaux, M. (2001). Water resource and power generation. *International Journal of Industrial Organization*, 19(6):975–997.

Cui, J., Lian, X., Huntingford, C., Gimeno, L., Wang, T., Ding, J., He, M., Xu, H., Chen, A., Gentine, P., et al. (2022). Global water availability boosted by vegetation-driven changes in atmospheric moisture transport. *Nature Geoscience*, 15(12):982–988.

Damania, R., Desbureaux, S., and Zaveri, E. (2020). Does rainfall matter for economic growth? evidence from global sub-national data (1990–2014). *Journal of Environmental Economics and Management*, 102:102335.

Dasgupta, P. (2021). *The economics of biodiversity: the Dasgupta review.* Hm Treasury.

De Faria, F. A., Davis, A., Severnini, E., and Jaramillo, P. (2017). The local socio-economic impacts of large hydropower plant development in a developing country. *Energy Economics*, 67:533–544.

Demarty, M. and Bastien, J. (2011). Ghg emissions from hydroelectric reservoirs in tropical and equatorial regions: Review of 20 years of ch4 emission measurements. *Energy Policy*, 39(7):4197–4206.

Edenhofer, O., Pichs-Madruga, R., Sokona, Y., Seyboth, K., Matschoss, P., Kadner, S., Zwickel, T., Eickemeier, P., Hansen, G., Schlömer, S., et al. (2011). Ipcc special report on renewable energy sources and climate change mitigation. *Prepared By Working Group III of the Intergovernmental Panel on Climate Change, Cambridge University Press, Cambridge, UK*.

EPA (2016). Social Cost of Carbon. *Environmental Protection Agency (EPA): Washington, DC, USA*.

Eyer, J. and Wichman, C. J. (2018). Does water scarcity shift the electricity generation mix toward fossil fuels? empirical evidence from the united states. *Journal of Environmental Economics and Management*, 87:224–241.

Fan, P., Cho, M. S., Lin, Z., Ouyang, Z., Qi, J., Chen, J., and Moran, E. F. (2022). Recently constructed hydropower dams were associated with reduced economic production, population, and greenness in nearby areas. *Proceedings of the National Academy of Sciences*, 119(8):e2108038119.

Fearnside, P. M. (2005). Do hydroelectric dams mitigate global warming? the case of brazil's curuá-una dam. *Mitigation and adaptation Strategies for Global change*, 10(4):675–691.

Ferraro, P. J., Lawlor, K., Mullan, K. L., and Pattanayak, S. K. (2020). Forest figures: Ecosystem services valuation and policy evaluation in developing countries. *Review of Environmental Economics and Policy*.

Ferreira, P. G. C., Oliveira, F. L. C., and Souza, R. C. (2015). The stochastic effects on the brazilian electrical sector. *Energy Economics*, 49:328–335.

Franklin Jr, S. L. and Pindyck, R. S. (2018). Tropical forests, tipping points, and the social cost of deforestation. *Ecological Economics*, 153:161–171.

Genc, T. S. and Thille, H. (2011). Investment in electricity markets with asymmetric technologies. *Energy Economics*, 33(3):379–387.

Grosset, F., Papp, A., and Taylor, C. (2023). Rain follows the forest: Land use policy, climate change, and adaptation. *Working paper*.

Guo, Z., Li, Y., Xiao, X., Zhang, L., and Gan, Y. (2007). Hydroelectricity production and forest conservation in watersheds. *Ecological Applications*, 17(6):1557–1562.

Halliday, D., Resnick, R., and Walker, J. (2013). *Fundamentals of physics*. John Wiley & Sons.

Hernandez-Cortes, D. and Meng, K. C. (2023). Do environmental markets cause environmental injustice? evidence from california's carbon market. *Journal of Public Economics*, 217:104786.

IEA, P. (2021). Hydropower special market report. *https://www.iea.org/reports/hydropower-special-market-report*.

IEMA, I. d. E. e. M. A. (2022). Inventário de emissões atmosféricas em usinas termelétricas.

Jahns, C., Podewski, C., and Weber, C. (2020). Supply curves for hydro reservoirs–estimation and usage in large-scale electricity market models. *Energy Economics*, 87:104696.

Johnson, J. A., Ruta, G., Baldos, U., Cervigni, R., Chonabayashi, S., Corong, E., Gavryliuk, O., Gerber, J., Hertel, T., Nootenboom, C., et al. (2021). *The Economic Case for Nature: A global Earth-economy model to assess development policy pathways*. World Bank.

Jung, S., Dyngeland, C., Rausch, L., and Rasmussen, L. V. (2022). Brazilian land registry impacts on land use conversion. *American Journal of Agricultural Economics*, 104(1):340–363.

Lawrence, D. and Vandecar, K. (2015). Effects of tropical deforestation on climate and agriculture. *Nature climate change*, 5(1):27–36.

Leite-Filho, A. T., Soares-Filho, B. S., Davis, J. L., Abrahão, G. M., and Börner, J. (2021). Deforestation reduces rainfall and agricultural revenues in the brazilian amazon. *Nature Communications*, 12(1):2591.

Mapbiomas (2022). Mapbiomas amazon project - collection 3. *amazonia.mapbiomas.org*, page acessed in 06/11/2022.

Marengo, J. A., Souza Jr, C. M., Thonicke, K., Burton, C., Halladay, K., Betts, R. A., Alves, L. M., and Soares, W. R. (2018). Changes in climate and land use over the amazon region: current and future variability and trends. *Frontiers in Earth Science*, 6:228.

Markit, I. (2021). Land price data for the year 2021. *IHS Markit Market Intelligence*.

Miller, N., Molitor, D., and Zou, E. (2017). Blowing smoke: Health impacts of wildfire plume dynamics. *Environmental And Resource Economics At The University Of Illinois*.

Mohai, P., Pellow, D., and Roberts, J. T. (2009). Environmental justice. *Annual review of environment and resources*, 34:405–430.

Moita, R. M. (2008). Entry and externality: Hydroelectric generators in brazil. *International Journal of Industrial Organization*, 26(6):1437–1447.

Nobre, C. A., Sellers, P. J., and Shukla, J. (1991). Amazonian deforestation and regional climate change. *Journal of climate*, 4(10):957–988.

Núñez, D., Nahuelhual, L., and Oyarzún, C. (2006). Forests and water: The value of native temperate forests in supplying water for human consumption. *Ecological economics*, 58(3):606–616.

Olmstead, S. M. (2020). The economics of managing scarce water resources. *Review of Environmental Economics and policy*.

Olmstead, S. M. and Sigman, H. (2015). Damming the commons: An empirical analysis of international cooperation and conflict in dam location. *Journal of the Association of Environmental and Resource Economists*, 2(4):497–526.

ONS (2022). Operador nacional do sistema elétrico. *www.ons.org.br*, page acessed in 06/11/2022.

Qiu, M., Ratledge, N., Azevedo, I., Diffenbaugh, N. S., and Burke, M. (2023). Drought impacts on the electricity system, emissions, and air quality in the western us. *Proceedings of the National Academy of Sciences*, 120(28):e2300395120.

Rosende, C., Sauma, E., and Harrison, G. P. (2019). Effect of climate change on wind speed and its impact on optimal power system expansion planning: The case of chile. *Energy Economics*, 80:434–451.

Salati, E., Dall'Olio, A., Matsui, E., and Gat, J. R. (1979). Recycling of water in the amazon basin: an isotopic study. *Water resources research*, 15(5):1250–1258.

Seneviratne, S., Nicholls, N., Easterling, D., Goodess, C., Kanae, S., Kossin, J., Luo, Y., Marengo, J., McInnes, K., Rahimi, M., et al. (2012). Changes in climate extremes and their impacts on the natural physical environment.

Shukla, J., Nobre, C., and Sellers, P. (1990). Amazon deforestation and climate change. *Science*, 247(4948):1322–1325.

Sigman, H. (2002). International spillovers and water quality in rivers: do countries free ride? *American Economic Review*, 92(4):1152–1159.

Simonet, G., Subervie, J., Ezzine-de Blas, D., Cromberg, M., and Duchelle, A. E. (2019). Effectiveness of a redd+ project in reducing deforestation in the brazilian amazon. *American Journal of Agricultural Economics*, 101(1):211–229.

Skidmore, M. (2022). Out-sourcing the dry season: cattle ranchers responses to weather shocks in the brazilian amazon. *Working paper*.

Smith, C., Baker, J., and Spracklen, D. (2023). Tropical deforestation causes large reductions in observed precipitation. *Nature*, 615(7951):270–275.

Souza-Rodrigues, E. (2019). Deforestation in the amazon: A unified framework for estimation and policy analysis. *The Review of Economic Studies*, 86(6):2713–2744.

Spracklen, D. V., Arnold, S. R., and Taylor, C. (2012). Observations of increased tropical rainfall preceded by air passage over forests. *Nature*, 489(7415):282–285.

Staal, A., Koren, G., Tejada, G., and Gatti, L. V. (2023). Moisture origins of the amazon carbon source region. *Environmental Research Letters*, 18(4):044027.

Staal, A., Tuinenburg, O. A., Bosmans, J. H., Holmgren, M., van Nes, E. H., Scheffer, M., Zemp, D. C., and Dekker, S. C. (2018). Forest-rainfall cascades buffer against drought across the amazon. *Nature Climate Change*, 8(6):539–543.

Stickler, C. M., Coe, M. T., Costa, M. H., Nepstad, D. C., McGrath, D. G., Dias, L. C., Rodrigues, H. O., and Soares-Filho, B. S. (2013). Dependence of hydropower energy generation on forests in the amazon basin at local and regional scales. *Proceedings of the National Academy of Sciences*, 110(23):9601–9606.

Wooldridge, J. M. (2005). Violating ignorability of treatment by controlling for too many factors. *Econometric Theory*, 21(5):1026–1028.

Wunderling, N., Staal, A., Sakschewski, B., Hirota, M., Tuinenburg, O. A., Donges, J. F., Barbosa, H. M., and Winkelmann, R. (2022). Recurrent droughts increase risk of cascading tipping events by outpacing adaptive capacities in the amazon rainforest. *Proceedings of the National Academy of Sciences*, 119(32):e2120777119.

WWAP, U. (2012). World water assessment programme: The united nations world water development report 4: Managing water under uncertainty and risk.

Zemp, D. C., Schleussner, C.-F., Barbosa, H. M., Hirota, M., Montade, V., Sampaio, G., Staal, A., Wang-Erlandsson, L., and Rammig, A. (2017). Self-amplified amazon forest loss due to vegetation-atmosphere feedbacks. *Nature communications*, 8(1):14681.

8 Appendix

Table 1: Climate Model

Month	(0)	(1)	(2)	(3)
Jan	0.950***	0.934***	1.131***	1.312***
	(0.018)	(0.019)	(0.013)	(0.018)
Feb	1.122***	1.133***	1.351***	1.392***
	(0.021)	(0.022)	(0.013)	(0.020)
Mar	0.850***	0.825***	0.975***	0.968***
	(0.021)	(0.023)	(0.012)	(0.015)
Apr	1.429***	1.377***	1.421***	1.339***
	(0.042)	(0.044)	(0.023)	(0.018)
May	1.302***	1.335***	2.000***	1.181***
	(0.037)	(0.038)	(0.024)	(0.023)
Jun	0.681***	0.612***	1.126***	0.247***
	(0.017)	(0.018)	(0.031)	(0.014)
Jul	0.385***	0.376***	0.897***	0.028***
	(0.013)	(0.015)	(0.030)	(0.009)
Aug	0.933***	0.901***	1.239***	0.995***
	(0.022)	(0.023)	(0.043)	(0.022)
Sep	1.223***	1.193***	1.360***	1.201***
	(0.025)	(0.027)	(0.020)	(0.018)
Oct	0.574***	0.542***	0.855***	0.750***
	(0.018)	(0.019)	(0.011)	(0.016)
Nov	0.633***	0.606***	0.949***	1.350***
	(0.022)	(0.023)	(0.013)	(0.013)
Dec	0.859***	0.833***	1.181***	1.442***
	(0.023)	(0.025)	(0.015)	(0.014)
N.obs	516,240	516,240	516,240	516,240
Month FE	Yes	Yes	Yes	No
Year FE	No	Yes	Yes	Yes
Pixel FE	No	No	Yes	No
Pixel-Month FE	No	No	No	Yes
Distance	Yes	Yes	Yes	Yes
R^2	0.82	0.83	0.86	0.88
R^2 (within)	0.21	0.21	0.26	0.17
R^2 (between)	-0.42	0.32	-0.30	0.47

This table shows the estimates of Expression 1, a regression of monthly rainfall on the upwind exposure to the forest. Each column presents a different specification with a different set of fixed effects. Every specification includes total distance of the back trajectory on land as a control. Number of observations: 516,240. *** means p-value < 0.01.

Table 2: Precipitation and River Flow

Parameter	(1)	(2)
β	0.052***	0.049***
	(0.002)	(0.007)
α	6.109***	6.196***
	(0.042)	(0.154)
Month FE	No	Yes
# obs	72	72
R^2	0.94	0.95

This table shows the estimates for Expression 2, the regression of the log of the monthly river flow on the 4 months cumulative rainfall. The effect of rainfall on river flow is captured by the parameter β. In column (2), I add a month fixed effect. Number of observations: 72. *** means p-value < 0.01.

Table 3: Data Description

Data	Description	Source
Wind speed and direction	Three dimensional (latitude, longitude, pressure) monthly data on wind speed and direction from 1985 to 2020 for South America at the resolution of 0.25°	Copernicus (2017)
Rainfall	Monthly data on precipitation from 1985 to 2020 for South America at the resolution of 0.25°. ERA5 reanalysis combines model data with global observations	Copernicus (2017)
Land use	Yearly data on land use for the entire Amazon Rainforest. Original resolution is of approximately 30 meters. It is then filtered (taking the average) to match the wind data resolution	Mapbiomas (2022)
River flow	Monthly data on river flow from 2015 to 2020 for the Teles Pires HP	ONS (2022)
Energy price	Monthly average of the price of energy – Price for Settlement of Differences (PLD) – from 2015 to 2020	CCEE (2022)

This table describes the data used in the paper and their sources.

Table 4: Descriptive Statistics

Month	Rainfall (mm)	River flow (m^3/s)	Energy price (USD/MW.h)	Forest exposure
Jan	9.37	2669.33	36.21	2.00
	(2.53)	(436.33)	(21.87)	(1.02)
Feb	9.43	3796.50	38.97	1.80
	(2.67)	(977.54)	(27.79)	(1.07)
Mar	7.97	4778.50	33.96	1.72
	(2.25)	(807.73)	(19.39)	(1.11)
Apr	4.74	4282.17	32.68	0.89
	(2.04)	(804.28)	(25.36)	(0.77)
May	1.63	2505.00	40.86	0.72
	(1.19)	(695.16)	(26.32)	(0.48)
Jun	0.34	1360.00	35.81	0.75
	(0.51)	(290.74)	(30.04)	(0.57)
Jul	0.20	850.83	41.40	0.82
	(0.36)	(179.42)	(28.76)	(0.64)
Aug	0.46	604.33	48.14	0.73
	(0.73)	(105.37)	(35.33)	(0.52)
Sep	1.96	503.83	50.76	0.99
	(1.52)	(97.47)	(31.62)	(0.76)
Oct	4.80	661.33	54.04	1.46
	(1.69)	(155.11)	(22.29)	(0.95)
Nov	7.13	989.00	53.70	2.010
	(2.05)	(290.78)	(30.67)	(0.96)
Dec	8.85	1893.00	32.48	2.10
	(2.42)	(846.45)	(16.13)	(0.89)

This table shows descriptive statistics (mean and standard deviation) of the data used in the paper by month. As the forest exposure is normalized by its standard deviation, it has no unit of measurement.